



## Reduced functional connectivity of default mode network subsystems in depression: Meta-analytic evidence and relationship with trait rumination

Leonardo Tozzi<sup>a</sup>, Xue Zhang<sup>a</sup>, Megan Chesnut<sup>a</sup>, Bailey Holt-Gosselin<sup>a</sup>, Carolina A. Ramirez<sup>a</sup>, Leanne M. Williams<sup>a,b,\*</sup>

<sup>a</sup> Department of Psychiatry and Behavioral Sciences, Stanford University, Stanford, USA

<sup>b</sup> Sierra-Pacific Mental Illness Research, Education, and Clinical Center (MIRECC) Veterans Affairs Palo Alto Health Care System, Palo Alto, CA, USA

### ARTICLE INFO

#### Keywords:

Resting state  
Functional MRI  
Default mode  
Depression  
Rumination  
Meta-analysis

### ABSTRACT

Resting-state functional connectivity changes in the default mode network (DMN) of patients with major depressive disorder (MDD) have been linked to rumination. The DMN is divided into three subsystems: a midline Core, a dorsal medial prefrontal cortex (DMPFC) subsystem, and a medial temporal lobe (MTL) subsystem. We examined resting-state functional connectivity within and between DMN subsystems in MDD and its association with rumination. First, we conducted a meta-analysis on a large multi-site dataset of 618 MDD and 683 controls to quantify the differences in DMN subsystem functional connectivity between MDD and controls. Second, we tested the association of DMN subsystem functional connectivity and rumination in a sample of 115 unmedicated participants with symptoms of anxiety/depression and 48 controls.

In our meta-analysis, only functional connectivity in the DMN Core was significantly reduced in MDD compared to controls ( $g = -0.246$ ,  $CI = [-0.417; -0.074]$ ,  $pFDR = 0.048$ ). Functional connectivity in the DMPFC subsystem and between the Core and DMPFC subsystems was slightly reduced but not significantly ( $g = -0.162$ ,  $CI = [-0.310; -0.013]$ ,  $pFDR = 0.096$ ;  $g = -0.249$ ,  $CI = [-0.464; -0.034]$ ,  $pFDR = 0.084$ ). Results were heterogeneous across sites for connectivity in the Core and between Core and DMPFC ( $I^2 = 0.348$  and  $I^2 = 0.576$  respectively). Prediction intervals consistently encompassed 0. In the independent sample we collected, functional connectivity within the DMN Core, DMPFC and between Core and DMPFC was not reduced in MDD compared to controls (all  $pFDR > 0.05$ ). Trait rumination did not predict connectivity within and between DMN subsystems (all  $pFDR > 0.05$ ).

We conclude that MDD as a diagnostic category shows slightly reduced functional connectivity within the DMN Core, independent of illness duration, treatment, symptoms and trait rumination. However, this effect is small, highly variable and heterogeneous across samples, so that we could only detect it at the meta-analytic level, with a sample size of several hundreds. Our results indicate that reduced Core DMN connectivity has significant limitations as a potential clinical or prognostic marker for the diagnosis of MDD and might be more relevant to consider as a characteristic distinguishing a subgroup of individuals within this diagnostic category.

### 1. Introduction

Major Depressive Disorder (MDD) is among the most prevalent mental diseases and it is the leading cause of disability worldwide (Friedrich, 2017). To make a dent in this burden of disease we urgently need to develop quantitative ways of identifying patients with MDD and to define different types of MDD. In doing so, we would have a means to more effectively tailor treatments and monitor their effectiveness.

Functional magnetic resonance imaging (fMRI) provides a non-

invasive approach to measuring brain activity under internal and external stimulations (Ogawa and Lee, 1990). Resting-state fMRI, in which data is collected in the absence of a task, has been used to measure spontaneous brain activity and has robustly identified large-scale brain networks of functionally connected regions (Thomas Yeo et al., 2011). Previous fMRI studies have reported resting-state functional connectivity changes in the default, salience and attention networks and in networks involved in cognitive control and emotional functions in patients with MDD (for review: (Brakowski et al., 2017; Williams, 2016;

\* Corresponding authors.

E-mail address: [leawilliams@stanford.edu](mailto:leawilliams@stanford.edu) (L.M. Williams).

<https://doi.org/10.1016/j.nicl.2021.102570>

Received 27 October 2020; Received in revised form 12 January 2021; Accepted 13 January 2021

Available online 18 January 2021

2213-1582/© 2021 The Authors.

Published by Elsevier Inc.

This is an open access article under the CC BY-NC-ND license

(<http://creativecommons.org/licenses/by-nc-nd/4.0/>).

Mulders et al., 2015), for meta-analysis: (Iwabuchi et al., 2015; Tang et al., 2018; Kaiser et al., 2015)). In particular, many studies have focused on the default mode network (DMN) (Williams, 2016; Zhou et al., 2020; Guo et al., 2014; Hamilton et al., 2015). The DMN is commonly defined by intrinsic functional connectivity between the posterior cingulate cortex, medial prefrontal cortex, superior parietal lobules and portions of the temporal and dorsomedial prefrontal cortex (Thomas Yeo et al., 2011; Greicius et al., 2007). A number of studies have reported hyper-connectivity between these regions (for review: (Williams, 2016; Mulders et al., 2015)), including a large meta-analysis comparing 556 medicated and unmedicated MDD with 518 controls (Kaiser et al., 2015). However, hypo-connectivity of the DMN has also been observed in the past (for review: (Williams, 2016)) and, most recently, in outcomes from the REST-meta-MDD Consortium. This Consortium undertook a multi-center study of 1300 treated and untreated MDD patients and 1128 healthy controls, and observed that DMN hypo-connectivity was characteristic of recurrent MDD in particular (Yan et al., 2019). This suggests that the previous findings in the literature may have been due to small and heterogeneous samples. As the dataset collected by the REST-meta-MDD Consortium is shared openly, it offers a chance to investigate functional alterations of the DMN in MDD more closely.

As advances are made in the precision with which resting intrinsic connectivity can be quantified, studies have moved from considering the DMN as a unitary network to revealing divergent functions of regions within the DMN. From these accumulating insights, the DMN may be conceptualized to encompass a broader network of at least three subsystems (Andrews-Hanna et al., 2010): 1) a midline Core, consisting of posterior cingulate cortex and anterior medial prefrontal cortex, which is hypothesized to integrate the function of the other subsystems and is involved in the introspection about one's own mental states (Andrews-Hanna et al., 2010); 2) a dorsal medial prefrontal cortex (DMPFC) subsystem, which includes the DMPFC, temporoparietal junction, lateral temporal cortex, and temporal pole, whose function is associated with mentalizing and metacognition (Ochsner et al., 2004); and 3) a medial temporal lobe (MTL) subsystem, consisting of ventral medial prefrontal cortex, posterior inferior parietal lobule, retrosplenial cortex, parahippocampal cortex and hippocampal formation, which increases its activity when participants make episodic decisions about their future (Andrews-Hanna et al., 2010). This expanded view of the DMN has not yet been used to identify whether MDD may be more precisely characterized by dysfunctions in these finer-grained subsystems. From the inverse perspective, it is also unknown whether the clinical symptoms heterogeneity of MDD may be explained by relationships with distinct dysfunctions of the DMN subsystems. One proposed mechanism by which specific MDD symptoms may arise from specific forms of DMN dysfunction is in relation to the construct of rumination (for review: (Hamilton et al., 2015), for meta-analysis: (Zhou et al., 2020; Mor and Winquist, 2002)). Rumination is the process of repeatedly focusing on symptoms of distress and the possible causes and consequences of these symptoms (Nolen-Hoeksema et al., 2008). It can enhance negative thinking, hamper problem-solving ability and is strongly associated with the psychopathology of depression (Mor and Winquist, 2002; Nolen-Hoeksema et al., 2008; Treynor et al., 2003). A recent meta-analysis consisting of 14 fMRI studies linking DMN subsystems to rumination highlighted prominent roles of the DMN Core and DMPFC subsystems (Zhou et al., 2020). Similarly, a very recent study induced a rumination state in healthy subjects and found that it was associated with an increased functional connectivity between the Core and MTL subsystem and a decreased functional connectivity between the Core and DMPFC subsystem. Interestingly, in this study, self-reports of subjects' rumination in everyday life (trait rumination) were found to be negatively correlated specifically with the Core-DMPFC functional connectivity (Chen et al., 2020). These findings indicate DMN connectivity dysfunction may give rise to specific aspects of rumination through at least three different subsystems and that such dysfunction in these

systems might relate to the expression of ruminative symptoms over a time span of days.

In the present study, we aimed to examine resting-state functional connectivity within and between the DMN Core, DMPFC and MTL subsystems in MDD and its association with rumination. To this end, two primary analyses were implemented. First, we conducted a meta-analysis on the very large multi-site REST-meta-MDD dataset. This allowed us to robustly quantify the differences in DMN subsystem functional connectivity between MDD and healthy controls as well as to derive effect sizes, heterogeneity and prediction intervals of these differences to inform future studies. Second, we tested the association of DMN subsystem functional connectivity and rumination using a sample of participants with symptoms of depression and anxiety derived from the Human Connectome Project for Disordered Emotional States (HCP-DES (Tozzi et al., 2020)). We hypothesized that resting-state functional connectivity within and between DMN subsystems would be lower in MDD and that it would correlate negatively with rumination levels.

## 2. Methods

Code to reproduce all the analyses (except preprocessing) is available at: [https://github.com/leotozzi88/dmn\\_subsystems](https://github.com/leotozzi88/dmn_subsystems).

### 2.1. Meta-analysis of default mode network subsystems connectivity in depression

#### 2.1.1. Data extraction

We downloaded the Meta-MDD dataset ([www.rfmri.org/REST-meta-MDD](http://www.rfmri.org/REST-meta-MDD)) and selected participants that were not excluded after the extensive quality checks documented in (Yan et al., 2019). This participant list was obtained from the Github repository of the Author of (Yan et al., 2019) ([https://github.com/Chaogan-Yan/PaperScripts/tree/master/Yan\\_2019\\_PNAS/StatsSubInfo](https://github.com/Chaogan-Yan/PaperScripts/tree/master/Yan_2019_PNAS/StatsSubInfo)). For our analysis, we used resting state BOLD timeseries extracted from Power atlas (Power et al., 2011) regions after these preprocessing steps: slice timing correction, realignment, nuisance covariates removed (six motion parameters, cerebrospinal fluid and white matter signals), spatial normalization, bandpass filtering (0.01–0.1 Hz) ((Yan, 2019) for details). Then, we extracted the timeseries of the 58 regions labeled as DMN based on the labels provided by the Author of (Power et al., 2011) at <http://www.jonathanpower.net/2011-neuron-bigbrain.html>. For each of the DMN regions, we obtained center of mass coordinates in MNI space. Then, we used the 17 networks version of the Yeo parcellation to assign each region to a DMN subsystem based on the location of the center of mass (Thomas Yeo et al., 2011; Chen et al., 2020; Andrews-Hanna, 2011). This returned the following number of regions for each subsystem: None: 9, Core: 21, DMPFC: 21, MTL: 7 (Fig. S1). To account for motion, we censored timepoints with > 0.25 mm framewise displacement from the timeseries and excluded subjects with > 25% of timepoints censored (Power et al., 2014). After all these steps, a total of 618 healthy controls and 683 depressed participants were retained (see Table 1 for participants' characteristics divided by site). As a measure of functional connectivity, we used the Pearson correlation coefficient between the timeseries, followed by the Fisher z-transformation. Finally, we computed the average functional connectivity within each subsystem and between each pair of subsystems, for a total of 6 subnetwork connectivity measures (within Core, within DMPFC, within MTL, Core-DMPFC, Core-MTL, and DMPFC-MTL) per participant.

#### 2.1.2. Meta-analysis procedure

We regressed out the effects of age and sex on functional connectivity for each subnetwork connectivity measure and site separately. Using the package "meta" in R version 3.6.3 for Mac, we ran four meta-analyses for each subnetwork connectivity measure to pool data across sites, excluding sites with less than 20 individuals per group. We tested the following effects: mean connectivity of MDD < Controls (N = 595 and

**Table 1**

Summary information for meta-analysis each site. We show demographic and clinical variables of interest as well as default mode network subsystem functional connectivity. For each variable, subjects with missing information were not counted and not included in the summary measures calculations. HC = healthy controls, MDD = major depressive disorder, SD = standard deviation, DMN = default mode network, DMPFC = dorsomedial prefrontal cortex, FC = functional connectivity, n. a. = no data available, HAMA = Hamilton anxiety scale, HAMD = Hamilton depression scale.

	Site														
	S01	S02	S07	S08	S09	S10	S11	S13	S14	S15	S17	S20	S21	S22	S23
N	100	25	60	84	90	51	36	35	87	61	71	409	120	32	40
N males	43	5	21	32	48	26	16	13	32	24	21	138	52	16	16
N females	57	20	39	52	42	25	20	22	55	37	50	271	68	16	24
N HC	48	11	31	47	46	20	17	16	31	35	37	188	55	18	18
N MDD	52	14	29	37	44	31	19	19	56	26	34	221	65	14	22
N recurrent	n.a.	8	9	2	24	n.a.	17	n.a.	n.a.	n.a.	n.a.	42	62	n.a.	8
N first onset	n.a.	6	20	34	20	30	2	n.a.	56	n.a.	n.a.	163	3	n.a.	14
N untreated	n.a.	1	7	31	43	n.a.	5	18	n.a.	n.a.	n.a.	101	n.a.	2	15
N treated	n.a.	12	22	6	1	n.a.	14	1	56	n.a.	n.a.	97	n.a.	12	7
Age mean	30.690	44.080	39.033	31.310	28.256	31.961	30.583	33.000	29.690	42.574	21.197	37.758	35.208	29.156	28.950
Age SD	7.764	12.007	11.763	10.264	8.190	9.071	9.361	9.299	6.102	14.303	2.556	13.507	12.449	9.870	9.682
HAMD median	24	22	22	24	n.a.	20	21	24	21	26	19	21	14	22	20
HAMA median	n.a.	n.a.	22	18	12	16	n.a.	n.a.	n.a.	15	22	13	8	n.a.	n.a.
DMN Core FC mean	0.399	0.348	0.341	0.388	0.348	0.345	0.343	0.303	0.318	0.311	0.387	0.376	0.373	0.309	0.308
DMN Core FC SD	0.109	0.091	0.100	0.107	0.106	0.090	0.123	0.104	0.085	0.085	0.090	0.097	0.087	0.091	0.073
DMN DMPFC FC mean	0.271	0.274	0.237	0.272	0.287	0.224	0.283	0.245	0.191	0.190	0.268	0.249	0.218	0.199	0.252
DMN DMPFC FC SD	0.083	0.079	0.081	0.080	0.100	0.074	0.077	0.096	0.067	0.073	0.077	0.080	0.083	0.076	0.077
DMN MTL FC mean	0.454	0.366	0.379	0.461	0.400	0.350	0.499	0.400	0.291	0.323	0.494	0.440	0.409	0.320	0.333
DMN MTL FC SD	0.151	0.098	0.131	0.150	0.116	0.123	0.123	0.142	0.105	0.105	0.137	0.134	0.115	0.127	0.122
DMN Core-DMPFC FC mean	0.239	0.236	0.212	0.242	0.240	0.217	0.239	0.205	0.181	0.187	0.233	0.237	0.222	0.181	0.200
DMN Core-DMPFC FC SD	0.085	0.067	0.070	0.083	0.092	0.070	0.098	0.087	0.067	0.072	0.072	0.074	0.076	0.068	0.066
DMN DMPFC-MTL FC mean	0.145	0.098	0.115	0.176	0.133	0.125	0.198	0.121	0.068	0.095	0.170	0.139	0.121	0.086	0.099
DMN DMPFC-MTL FC SD	0.098	0.097	0.075	0.095	0.086	0.067	0.089	0.091	0.055	0.065	0.093	0.075	0.073	0.064	0.053
DMN MTL-Core FC mean	0.280	0.200	0.227	0.303	0.248	0.239	0.305	0.218	0.173	0.211	0.309	0.254	0.256	0.205	0.190
DMN MTL-Core FC SD	0.114	0.090	0.090	0.110	0.084	0.076	0.113	0.100	0.062	0.086	0.097	0.089	0.084	0.078	0.058

538), Spearman correlations between connectivity and depression severity across all subjects (total Hamilton depression scale; HAMD,  $N = 1083$ ) (Hamilton et al., 1986) and anxiety (Hamilton anxiety scale; HAMA,  $N = 885$ ) (Hamilton, 1959). Meta-analyses were random-effects models using the Hartung-Knapp method and  $\tau$  estimation using REML (Veroniki et al., 2016). Thus, we obtained estimates of the effect size of our effects across sites (Hedges  $g$ ), prediction intervals (effects that can be expected in future settings), square standard deviation of between-study effects ( $\tau^2$ ), inconsistency between study results ( $I^2$ ) and heterogeneity of results (Cochrane  $Q$ ) (Schwarzer et al., 2020). We corrected  $p$ -values for multiple comparisons using false discovery rate (FDR) across DMN subsystems connectivity measures.

### 2.1.3. Effects of recurrence

In (Yan et al., 2019), the Authors reported that DMN functional connectivity differences between MDD and controls were driven by recurrent patients. To test whether this was true of DMN subsystem connectivity, we tested whether the 3 functional connectivity measures that we found to be decreased in MDD with a confidence interval not encompassing 0 in the meta-analysis (Core, DMPFC and Core-DMPFC) were driven by recurrent patients. Only one site of the Meta-MDD dataset had more than 20 patients with information about recurrence (S20). Therefore, we conducted  $t$ -tests on patients within this site

comparing recurrent ( $N = 42$ ) and first episode patients ( $N = 163$ ).

### 2.1.4. Effects of confounds

To assess the impact of motion on our results, we conducted a meta-analysis on the correlation between the number of volumes containing critical motion and our functional connectivity measures as described above ( $N = 1301$ ). Also, we compared the number of censored time-points between MDD and controls using a Mann-Whitney  $U$  test.

We also conducted a meta-analysis on the correlation between age and our functional connectivity measures ( $N = 1301$ ) and a meta-analysis comparing males and females ( $N = 503$  and  $798$  respectively) for our functional connectivity measures as described above.

Only one site of the Meta-MDD dataset had more than 20 patients on medication and 20 patients not on medication (S20). Therefore, we conducted  $t$ -tests on patients within this site comparing medicated ( $N = 97$ ) and unmedicated patients ( $N = 101$ ).

## 2.2. Default mode network subsystems connectivity and rumination

### 2.2.1. Study design

The second part of the study was conducted on a sample of participants from the Human Connectome Project for Disordered Emotional States (HCP-DES). Details about the study design and measures of HCP-

DES are available at (Tozzi et al., 2020). Here only the measures relevant to the current analysis will be presented.

### 2.2.2. Participants

Our sample consisted of 76 healthy controls (HC) and 133 unmedicated clinical participants with symptoms of depression and/or anxiety between 18 and 35 years of age. Participants were recruited from the surrounding community using flyers and social media advertisements (i.e., Facebook and Instagram Ads). All participants responded to an online screening survey reviewed by a study coordinator to determine eligibility. The survey included demographics, any current or past pharmacotherapy or psychotherapy, medical history, MRI scanner contraindications, anxiety and depression symptoms, and alcohol or substance use. To assess eligibility, levels of clinical symptoms were assessed by an in-house screening survey composed of five categories (containing four items in each) selected to match each of the four constructs identified using a factor analysis of data from (Grisanzio et al., 2018): anhedonia, anxious arousal, concentration, rumination, and tension. In order to be classified as a clinical participant, respondents had to report that at least one symptom related statement “often” or “almost always/always” applied to them in the last two weeks and indicate that the symptoms caused significant distress and/or impairment in everyday life. In order to be classified as a healthy control, respondents had to report that symptom-related statements applied to them only “occasionally” or “rarely/never” in the last two weeks and indicate that any symptoms they may have experienced did not cause significant distress or impairment. Further, clinical and healthy control participants were allowed to participate only if they were not taking any psychotropic medications for a mental health problem (i.e., SSRIs, benzodiazepines, etc.) or receiving therapy by a trained mental health professional (social worker, clinical psychologist, psychiatrist, etc.) and if they had no contraindications for MRI scanning. Eligible participants then proceeded to an on-site visit during which questionnaires, behavioral testing and MRI imaging were conducted.

### 2.2.3. Assessments

We administered the Mini-International Neuropsychiatric Interview (MINI-Plus) to assess mood and anxiety disorders based on Diagnostic and Statistical Manual of Mental Disorders (DSM-5) criteria. According to their DSM diagnoses, clinical participants were divided into 3 groups: diagnosis of current major depressive disorder (MDD), diagnosis of any current anxiety disorder (generalized anxiety, social anxiety, panic disorder) and diagnosis of both current MDD and any anxiety disorder.

To quantify rumination, we administered the Ruminative Responses Scale (RRS), a 22-item self-report questionnaire. For our analyses, we used the total score of the questionnaire and its three subscales: brooding, depression related and reflection (Parola et al., 2017).

### 2.2.4. Neuroimaging acquisition details

Images were acquired at the Stanford Center for Cognitive and Neurobiological Imaging (CNI) on a GE Discovery MR750 3 T scanner using a Nova Medical 32-channel head coil. Two spin-echo fieldmaps were acquired at the beginning of each session, one with a posterior-anterior phase encoding direction, the other with an anterior-posterior direction. All fMRI scans were conducted using a blipped-CAIPI simultaneous multislice “multiband” acquisition (Setsompop et al., 2012).

1. Spin-echo fieldmaps: TE = 55.5 ms, TR = 6 s, FA = 90°, acquisition time = 18 s, field of view = 220.8 × 220.8 mm, 3D matrix size = 92 × 92 × 60, slice orientation = axial, angulation to anterior commissure - posterior commissure (AC-PC) line, phase encoding = AP and PA, receiver bandwidth = 250 kHz, readout duration = 49.14 ms, echo spacing = 0.54 ms, voxel size = 2.4 mm isotropic.
2. Single-band calibration: TE = 30 ms, TR = 4.4 s, FA = 90°, acquisition time = 13 s, field of view = 220.8 × 220.8 mm, 3D matrix size = 92 × 92 × 60, slice orientation = axial, angulation to AC-PC line,

phase encoding = PA, receiver bandwidth = 250 kHz, readout duration = 49.14 ms, echo spacing = 0.54 ms, number of volumes = 4, voxel size = 2.4 mm isotropic.

3. Multiband fMRI: TE = 30 ms, TR = 0.71 s, FA = 54°, acquisition time = 5: 12 (rest), field of view = 220.8 × 220.8 mm, 3D matrix size = 92 × 92 × 60, slice orientation = axial, angulation to AC-PC line, phase encoding = PA, receiver bandwidth = 250 kHz, readout duration = 49.14 ms, echo spacing = 0.54 ms, number of volumes for rest-state run = 440, multiband factor = 6, calibration volumes = 2, voxel size = 2.4 mm isotropic.
4. T1-weighted: TE = 3.548 ms, MPRAGE TR = 2.84 s, FA = 8°, acquisition time = 8: 33, field of view = 256 × 256 mm, 3D matrix size = 320 × 320 × 230, slice orientation = sagittal, angulation to AC-PC line, receiver bandwidth = 31.25 kHz, fat suppression = no, motion correction = PROMO, voxel size = 0.8 mm isotropic.
5. T2-weighted: TE = 74.4 ms, TR = 2.5 s, FA = 90°, acquisition time = 5: 42, field of view = 240 × 240 mm, 3D matrix size = 320 × 320 × 216, slice orientation = sagittal, angulation to AC-PC line, receiver bandwidth = 125 kHz, fat suppression = no, motion correction = PROMO, voxel size = 0.8 mm isotropic.

### 2.2.5. Resting state paradigm

Participants were instructed to stare at a white cross on a black background. During this time, their eyes were monitored using an eye-tracker by the study coordinator to ensure that the participant was asleep. Four separate 5:12 runs of resting state data were acquired.

### 2.2.6. Preprocessing

Raw image files were converted to BIDS format and preprocessed using fMRIPrep (Esteban et al., 2019). See Supplemental Material for the fMRIPrep boilerplate containing the details of the preprocessing stream. Briefly, brain surfaces were reconstructed using recon-all (FreeSurfer 6.0.1) (Dale et al., 1999). Susceptibility distortion for fMRI data were corrected using the two echo-planar imaging (EPI) references with opposing phase-encoding directions (Cox and Hyde, 1997). Surface data was registered to fsaverage space and subcortical data to MNI space. These were then merged to grayordinate CIFTI files. Automated labeling of noise components following ICA decomposition was performed using AROMA (Pruim et al., 2015). As final output, we down-sampled the preprocessed grey-ordinate functional CIFTI files to 32 k FSLR space (Glasser et al., 2013). Then, we applied a 4 mm full-width half-maximum smoothing constrained to the grey matter boundaries.

### 2.2.7. Functional connectivity

The confound regressors identified by AROMA were regressed from the timeseries of all grayordinates of the resting state fMRI CIFTIs. Then, we parcellated the resulting CIFTIs by averaging timeseries within the parcels of the Schaefer 300 parcellation, which provides labels corresponding to the Yeo 17 networks parcellation (Thomas Yeo et al., 2011; Schaefer et al., 2018). The number of parcels corresponding to the DMN subsystems were: core: 23, DMPFC: 58, MTL: 25 (Fig. S2). Mean timeseries from each parcel were extracted and high-pass filtered at 0.008 Hz. Then, we censored timepoints that had a framewise displacement > 0.25 mm (Power et al., 2014). If more than 25% of the timeseries was censored, the subject was excluded. Finally, we only considered participants with all the clinical variables of interest. This led to a final sample size of 163 participants (Table 2). The four runs of resting state were concatenated. Then, we computed Pearson correlations between the timeseries and applied a Fisher-z transformation. Finally, we computed the average functional connectivity within each subsystem and across each pair of subsystems, for a total of 6 subnetwork connectivity measures (within Core, within DMPFC, within MTL, Core-DMPFC, Core-MTL, and DMPFC-MTL) per participant. To assess if concatenating resting state runs before correlating timeseries was impacting our results, we also generated an alternative set of connectivity matrices by computing Pearson correlations for each run

**Table 2**

HCP-DES sample information. We show summary demographic and clinical variables of interest for the control and clinical group. SD = standard deviation, MDD = major depressive disorder, AnxD = anxiety disorder, DASS = Depression Anxiety Stress Scales, RRS = ruminative response scale.

	HC	Clinical
N total	48	115
N current MDD only	0	11
N current AnxD only	0	50
N current AnxD + MDD	0	30
N no current AnxD + no current MDD	48	24
Age (mean)	27.441	25.585
Age (SD)	4.971	4.902
DASS depression (median)	1	14
DASS anxiety (median)	1	8
DASS stress (median)	1	16
RRS total (median)	28	59
RRS brooding (median)	6	13
RRS depression related	14	33
RRS reflection (median)	6	13

separately, applying a Fisher-z transformation and averaging the resulting 4 matrices for each participant. We repeated all our analyses using this second set of matrices.

### 2.2.8. Confirmation of meta-analysis results

First, we attempted to confirm the results of the meta-analysis in the HCP-DES sample. We chose the 3 functional connectivity measures that we found to be decreased in MDD with a confidence interval not encompassing 0: Core, DMPFC and Core-DMPFC. Before conducting group comparisons, we regressed age and sex from all connectivity measures.

Since our sample was comprised of several participants with comorbid MDD and anxiety disorders, we used two strategies to divide them into two groups. First, we compared functional connectivity measures between participants with a diagnosis of current MDD or any anxiety disorder ( $N = 30$ ) versus people without current MDD or any anxiety disorder ( $N = 133$ ). Then, we compared the same measures between participants with ( $N = 122$ ) and without current MDD ( $N = 41$ ). We used one sided t-tests for these comparisons, correcting p-values using FDR.

### 2.2.9. Relationship with rumination

To test whether rumination would predict functional connectivity measures, we ran 24 linear regressions across all HCP-DES participants. Each regression had as predictors age, sex, a group factor (two possibilities as described above: current MDD/anxiety disorder versus neither MDD nor anxiety disorder or current MDD versus no current MDD), a rumination measure (RRS total, brooding, reflection and depression related) and the interaction between group and rumination measure. The dependent variables were the Core, DMPFC and Core-DMPFC connectivity respectively. We tested the significance of all the main effects and of the interaction in these linear regressions using t-tests and corrected the respective p-values using FDR.

We also tested whether we could identify subsystems of the DMN correlating with rumination that did not overlap with the ones we defined previously. To do so, we ran exploratory analyses using network-based statistics (NBS) (Zalesky et al., 2010). Network-based statistics is an approach that allows to identify correlations in any set of connected structures forming a graph of nodes and edges. In our case, we wanted to study the correlation of our rumination measures (RRS total, brooding, reflection and depression related) with the functional connectivity (edge values) between all regions (nodes) within the DMN. This is implemented in the following 6 steps. 1) The NBS procedure fits a general linear model predicting each edge value across all subjects with the following predictors: age, sex and total RRS. 2) A t-test for the effect of the RRS scale (beta value) is computed for each edge independently.

3) The test statistic is thresholded at each edge to form a set of supra-threshold edges. We tested all t-thresholds between 1 and 5 with a step of 0.2. 4) For each set, the sum of absolute t values is computed (“intensity”). 5) Steps 1–4 are repeated 10,000 times, each time randomly permuting the values of the predictors and storing the size and intensity of the largest component identified for each permutation. This yields an empirical estimate of the null distribution of maximal component intensity. 6) A corrected p-value for the effect of RRS is then calculated using this null distribution. The significance threshold was  $p < 0.05$ , FDR corrected for multiple comparisons across the number of components identified.

### 2.3. Ethical approval

For the Meta-MDD dataset, de-identified and anonymized data were contributed from studies approved by local Institutional Review Boards. All study participants provided written informed consent at their local institution.

The Institutional Review Boards of Stanford University has approved the HCP-DES protocol (protocol #41837). A study coordinator thoroughly explained the protocol to participants and answered any questions before they provided informed consent to begin the study. The study was conducted according to the principles of the Declaration of Helsinki (2008).

## 3. Results

### 3.1. Meta-analysis of default mode network subsystems connectivity in depression

All meta-analysis results are shown in Table 3.

#### 3.1.1. Effects of diagnosis

Functional connectivity in the DMN Core was reduced in MDD compared to controls ( $g = -0.246$ ,  $CI = [-0.417; -0.074]$ ,  $pFDR = 0.048$ , Fig. 1). Functional connectivity in the DMN DMPFC subsystem was also reduced, albeit not significantly ( $g = -0.162$ ,  $CI = [-0.310; -0.013]$ ,  $pFDR = 0.096$ , Fig. 2). The same was true for functional connectivity between the Core and DMPFC subsystems ( $g = -0.249$ ,  $CI = [-0.464; -0.034]$ ,  $pFDR = 0.084$ , Fig. 3). Results were heterogeneous across sites for DMN Core connectivity and connectivity between Core and DMPFC ( $I^2 = 0.348$  and  $I^2 = 0.576$  respectively).

These functional connectivity measures were especially lower in MDD compared to controls at one site (S09). Repeating the meta-analysis after excluding this site returned slightly weaker but similar results for the connectivity of the DMN Core ( $g = -0.155$ ,  $CI = [-0.270; -0.041]$ ,  $pFDR = 0.042$ ). After removing this site, confidence intervals encompassed 0 for the DMPFC ( $g = -0.123$ ,  $CI = [-0.248; 0.001]$ ,  $pFDR = 0.078$ ) and for the Core-DMPFC connectivity ( $g = -0.161$ ,  $CI = [-0.322; 0]$ ,  $pFDR = 0.130$ ).

Effects for correlations of symptom severity and illness duration with functional connectivity were non-significant and always encompassed 0. Also, prediction intervals encompassed 0 for all effects.

#### 3.1.2. Effects of recurrence

There was no significant difference between recurrent and first episode MDD in Core functional connectivity ( $t = -1.293$ ,  $df = 62.131$ ,  $p = 0.201$ ), DMPFC functional connectivity ( $t = -1.201$ ,  $df = 65.424$ ,  $p = 0.234$ ) and Core-DMPFC functional connectivity ( $t = -1.644$ ,  $df = 60.852$ ,  $p = 0.105$ ).

#### 3.1.3. Effects of confounds

Motion (number of removed frames) was significantly correlated to functional connectivity within the DMPFC and MTL subsystems ( $g = 0.103$ ,  $CI = [0.045; 0.162]$ ,  $pFDR = 0.016$  and  $g = 0.098$ ,  $CI = [0.040-0.157]$ ,  $pFDR = 0.018$ ) (Table S1). It was also significantly

**Table 3**

Meta-analysis results. For each effect of interest, we show effect size, confidence and prediction intervals, as well as measures of variability. MDD = major depressive disorder, HC = healthy controls, HAMD = Hamilton depression scale, HAMA = Hamilton anxiety scale, DMN = default mode network, DMPFC = dorsomedial prefrontal cortex, MTL = middle temporal lobe, FDR = false discovery rate.

Effect	Subsystem	MDD	HC	Effect (g)	Lower CI	Upper CI	Effect p	Effect pFDR	Lower PI	Upper PI	$\tau^2$	q	q p	q pFDR	I <sup>2</sup>
Mean MDD < HC	Core	595	538	-0.246	-0.417	-0.074	0.010	0.048	-0.641	0.150	0.024	13.809	0.129	0.207	0.348
	DMPFC	595	538	-0.162	-0.310	-0.013	0.036	0.096	-0.380	0.056	0.005	9.933	0.356	0.453	0.094
	MTL	595	538	-0.098	-0.227	0.032	0.122	0.244	-0.312	0.117	0.005	7.920	0.542	0.602	0.000
	Core-DMPFC	595	538	-0.249	-0.464	-0.034	0.028	0.084	-0.814	0.316	0.051	21.214	0.012	0.035	0.576
	Core-MTL	595	538	-0.135	-0.284	0.014	0.070	0.153	-0.368	0.098	0.006	9.899	0.359	0.453	0.091
	DMPFC-MTL	595	538	-0.169	-0.352	0.015	0.067	0.153	-0.584	0.247	0.026	14.257	0.113	0.195	0.369
Correlation with HAMD	Core	1083		0.035	-0.157	0.227	0.689	0.861	-0.521	0.592	0.051	36.986	0.000	0.001	0.757
	DMPFC	1083		-0.013	-0.100	0.075	0.753	0.861	-0.190	0.165	0.004	12.165	0.204	0.306	0.260
	MTL	1083		-0.001	-0.128	0.126	0.987	0.987	-0.325	0.323	0.017	21.792	0.010	0.035	0.587
	Core-DMPFC	1083		0.031	-0.116	0.179	0.641	0.855	-0.375	0.437	0.027	27.453	0.001	0.009	0.672
	Core-MTL	1083		-0.029	-0.155	0.097	0.611	0.855	-0.361	0.302	0.018	21.478	0.011	0.035	0.581
	DMPFC-MTL	1083		-0.034	-0.155	0.087	0.541	0.837	-0.319	0.251	0.012	18.296	0.032	0.085	0.508
Correlation with HAMA	Core	885		0.039	-0.099	0.177	0.516	0.837	-0.243	0.321	0.009	11.308	0.079	0.146	0.469
	DMPFC	885		0.042	-0.052	0.135	0.316	0.583	-0.090	0.174	0.001	6.789	0.341	0.453	0.116
	MTL	885		0.015	-0.137	0.166	0.822	0.878	-0.307	0.336	0.012	12.660	0.049	0.117	0.526
	Core-DMPFC	885		0.045	-0.134	0.224	0.558	0.837	-0.397	0.488	0.024	18.224	0.006	0.029	0.671
	Core-MTL	885		0.017	-0.178	0.212	0.841	0.878	-0.454	0.487	0.027	18.057	0.006	0.029	0.668
	DMPFC-MTL	885		0.030	-0.181	0.241	0.743	0.861	-0.512	0.572	0.037	22.924	0.001	0.009	0.738
Correlation with illness duration	Core	1102		-0.007	-0.148	0.135	0.918	0.918	-0.388	0.374	0.023	25.833	0.002	0.918	0.652
	DMPFC	1102		0.112	0.003	0.221	0.045	0.136	-0.172	0.396	0.013	21.139	0.012	0.136	0.574
	MTL	1102		0.050	-0.059	0.158	0.326	0.490	-0.208	0.307	0.010	17.200	0.046	0.490	0.477
	Core-DMPFC	1102		0.050	-0.055	0.155	0.311	0.583	-0.222	0.322	0.012	19.186	0.024	0.024	0.531
	Core-MTL	1102		0.052	-0.077	0.180	0.388	0.583	-0.290	0.393	0.019	26.717	0.002	0.005	0.663
	DMPFC-MTL	1102		-0.021	-0.125	0.084	0.666	0.666	-0.291	0.249	0.012	20.184	0.017	0.024	0.554

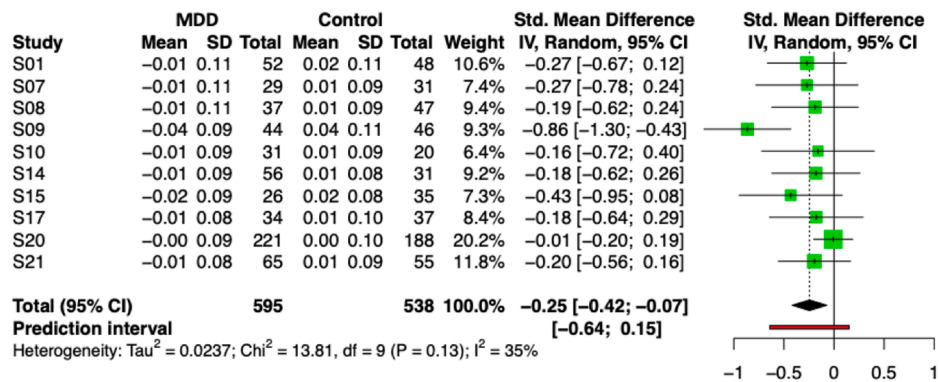


**Fig. 1.** Forest plot of meta-analysis results comparing Core functional connectivity between MDD and controls. MDD = major depressive disorder, SD = standard deviation, IV = inverse variance, CI = confidence interval.

correlated to connectivity between the MTL and Core as well as MTL and DMPFC subsystems ( $g = 0.131$ ,  $CI = [0.074; 0.189]$ ,  $pFDR = 0.003$  and  $g = 0.192$ ,  $CI = [0.147; 0.236]$ ,  $pFDR < 0.001$ ) (Table S1). The number of volumes containing critical motion did not differ between MDD and controls ( $W = 212,577$ ,  $p$ -value = 0.82).

On average, males compared to females had less connectivity within the DMPFC subsystem and more in the MTL subsystem ( $g = -0.174$ ,  $CI = [-0.330; -0.019]$ ,  $pFDR = 0.046$  and  $g = 0.234$ ,  $CI = [0.110-0.357]$ ,

$pFDR = 0.004$ ) (Table S1).

Age was not significantly correlated with any connectivity measure (all  $pFDR > 0.05$ ) (Table S1).

We found no significant difference between treated and untreated MDD in Core functional connectivity ( $t = 1.264$ ,  $df = 188.07$ ,  $p = 0.208$ ), DMPFC functional connectivity ( $t = 1.097$ ,  $df = 195.06$ ,  $p = 0.274$ ) and Core-DMPFC functional connectivity ( $t = 0.900$ ,  $df = 195.56$ ,  $p = 0.369$ ).

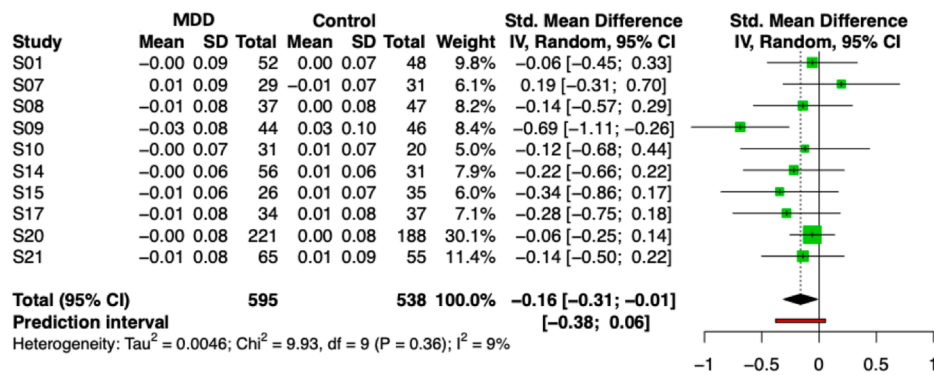


Fig. 2. Forest plot of meta-analysis results comparing DMPFC functional connectivity between MDD and controls. MDD = major depressive disorder, SD = standard deviation, IV = inverse variance, CI = confidence interval.

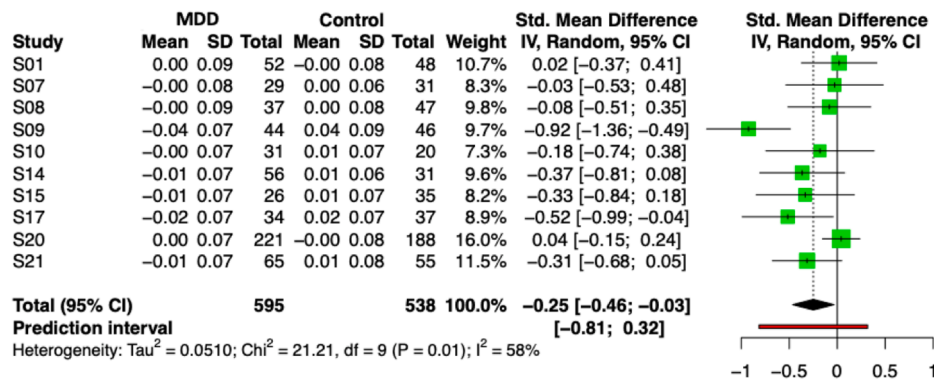


Fig. 3. Forest plot of meta-analysis results comparing Core to DMPFC subsystems functional connectivity between MDD and controls. MDD = major depressive disorder, SD = standard deviation, IV = inverse variance, CI = confidence interval.

### 3.2. Default mode network subsystems connectivity and rumination

#### 3.2.1. Confirmation of meta-analysis results

First, we compared participants with current MDD or any anxiety disorder versus people without current MDD or any anxiety disorder. Functional connectivity within the Core and DMPFC was reduced on average, but not significantly ( $t = -0.934$ ,  $\text{df} = 44.217$ ,  $\text{pFDR} = 0.230$  and  $t = -0.744$ ,  $\text{df} = 47.284$ ,  $\text{pFDR} = 0.230$ ) (Table 4, Fig. 4). Effect sizes were lower than the ones found in the meta-analysis ( $d = 0.184$  and  $d = 0.139$ ). Similarly, functional connectivity between the Core and DMPFC was reduced, but not significantly ( $t = -0.987$ ,  $\text{df} = 48.369$ ,  $\text{pFDR} = 0.230$ ). The effect size was  $d = 0.181$  (Table 4, Fig. 4).

Results comparing participants with current MDD versus people without current MDD were similar. Functional connectivity within the Core and DMPFC was reduced but not significantly ( $t = -1.161$ ,  $\text{df} = 75.613$ ,  $\text{pFDR} = 0.188$  and  $t = -0.734$ ,  $\text{df} = 83.015$ ,  $\text{pFDR} = 0.120$ ) (Table 4, Fig. 5), with effect sizes lower than the ones from the meta-analysis ( $d = 0.199$  and  $d = 0.120$ ). Like for the previous group

Table 4

Results of group comparisons in the HCP-DES sample. T-tests were adjusted by age and sex. DMN = default mode network, DMPFC = dorsomedial prefrontal cortex, FC = functional connectivity, MDD = major depressive disorder, AnxD = any anxiety disorder, FDR = false discovery rate, HCP-DES = human connectome project for disordered emotional states.

Group comparison	Subsystem	HC mean FC (SD)	MDD mean FC (SD)	t	df	p	pFDR	d
MDD or AnxD < No MDD or AnxD	DMN Core	0.316 (0.075)	0.303 (0.070)	-0.934	44.217	0.178	0.230	0.184
	DMN DMPFC	0.246 (0.081)	0.241 (0.073)	-0.744	47.284	0.230	0.230	0.139
	DMN Core-DMPFC	0.189 (0.068)	0.182 (0.059)	-0.987	48.369	0.164	0.230	0.181
MDD < No MDD	DMN Core	0.317 (0.076)	0.303 (0.067)	-1.161	75.613	0.125	0.188	0.199
	DMN DMPFC	0.246 (0.083)	0.242 (0.068)	-0.734	83.015	0.233	0.233	0.120
	DMN Core-DMPFC	0.190 (0.070)	0.180 (0.053)	-1.204	90.971	0.116	0.188	0.189

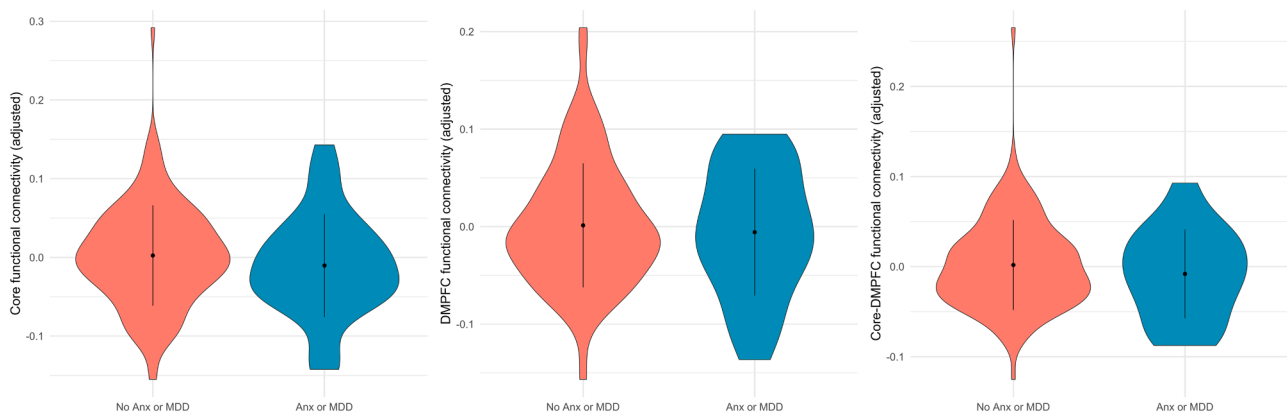


**Fig. 4.** Default mode network subsystem functional connectivity differences between participants with MDD or an anxiety disorder versus participants without MDD or an anxiety disorder in the HCP-DES sample. We show mean and standard deviation (dot and whiskers) for each group. Functional connectivity was adjusted by age and sex. Anx = Anxiety, MDD = major depressive disorder, DMPFC = dorsomedial prefrontal cortex, HCP-DES = human connectome project for disordered emotional states.

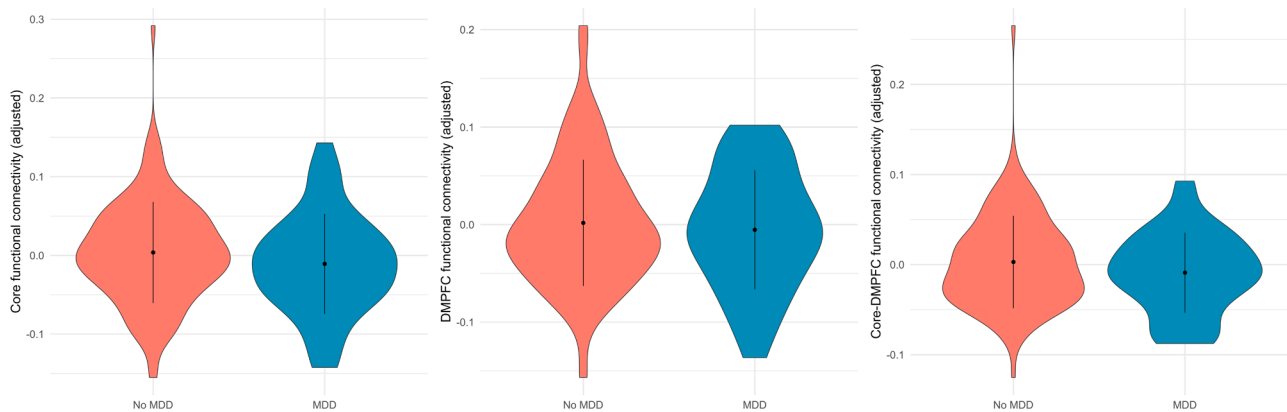


**Fig. 5.** Default mode network subsystem functional connectivity differences between participants with and without MDD in the HCP-DES sample. We show mean and standard deviation (dot and whiskers) for each group. Functional connectivity was adjusted by age and sex. MDD = major depressive disorder, DMPFC = dorsomedial prefrontal cortex, HCP-DES = human connectome project for disordered emotional states.

### 3.2.3. Results using connectivity matrices derived from non-concatenated timeseries

The alternative set of HCP-DES connectivity matrices obtained by correlating timeseries of each run and then averaging them for each participant generated comparable results.

Participants with current MDD or any anxiety disorder versus people without current MDD or any anxiety disorder did not show a significant reduction in connectivity of the Core or DMPFC ( $t = -0.967$ ,  $df = 42.397$ ,  $pFDR = 0.255$  and  $t = -0.536$ ,  $df = 42.420$ ,  $pFDR = 0.297$ ). Effect sizes were lower than the ones found in the meta-analysis ( $d = 0.198$  and  $d = 0.110$ ). Similarly, functional connectivity between the Core and DMPFC was reduced, but not significantly ( $t = -0.993$ ,  $df = 43.467$ ,  $pFDR = 0.255$ ,  $d = 0.199$ ) (Table S2).

For participants with current MDD versus without current MDD, functional connectivity within the Core and DMPFC was not significantly reduced ( $t = -1.260$ ,  $df = 69.518$ ,  $pFDR = 0.159$ ,  $d = 0.226$  and  $t = -0.632$ ,  $df = 72.543$ ,  $pFDR = 0.265$ ,  $d = 0.111$ ). Functional connectivity between Core and DMPFC was also not significantly reduced ( $t = -1.424$ ,  $df = 78.719$ ,  $pFDR = 0.159$ ,  $d = 0.239$ ) (Table S2).

We also found no significant effects of RRS total or subscales in predicting our 3 network measures, nor of their interaction with our group variables (all  $pFDR > 0.05$ ). See Table S3 for regression results using current MDD/anxiety disorder versus neither MDD nor anxiety disorder and Table S4 for regression results using current MDD versus no current MDD.

The exploratory analysis using network-based statistics also did not find any DMN subnetworks whose intensity correlated to the RRS total or subscales at any t-value threshold.

## 4. Discussion

In the present study, we provide meta-analytic evidence that reduced resting state DMN functional connectivity in MDD is localized within its Core subsystem, although this effect is small and has large variability as well as heterogeneity across sites. Contrary to our hypothesis, trait rumination does not significantly predict connectivity within and between DMN subsystems.

Our results expand on a previous study conducted on the Meta-MDD dataset, which found reduced DMN connectivity in MDD, driven by recurrent patients (Yan et al., 2019). This study also found that connectivity was reduced on average across sites within all three DMN subsystems as well as between the Core-DMPFC and Core-MTL subsystems (Yan et al., 2019). Our first novel contribution is to demonstrate in a meta-analysis that functional connectivity is robustly reduced across sites only within the Core subsystem of the DMN. This is in line also with previous studies that found decreased connectivity of MDD patients compared to controls in the DMN Core (Chen et al., 2015). It is worth noting that in the meta-analysis functional connectivity within the DMPFC subsystem and between the DMN Core and DMPFC subsystems was also slightly reduced in MDD compared to controls, with a



**Table 5**

Results of linear regressions predicting DMN subsystem connectivity from rumination in the HCP-DES sample considering current MDD or AnxD as a predictor. DMN = default mode network, DMPFC = dorsomedial prefrontal cortex, FC = functional connectivity, HC = healthy controls, MDD = major depressive disorder, AnxD = any anxiety disorder, FDR = false discovery rate, HCP-DES = human connectome project for disordered emotional states.

	DMN Core FC					DMN DMPFC FC					DMN Core-DMPFC FC				
	Coefficient	SE	t	p	pFDR	Coefficient	SE	t	p	pFDR	Coefficient	SE	t	p	pFDR
Sex	0.001	0.013	0.074	0.941	0.973	-0.021	0.014	-1.525	0.129	0.533	-0.025	0.011	-2.195	0.030	0.420
Age	-0.001	0.001	-0.812	0.418	0.791	-0.003	0.001	-1.971	0.051	0.437	-0.001	0.001	-0.519	0.604	0.791
RRS total	0.000	0.000	0.653	0.515	0.791	0.000	0.000	0.666	0.506	0.791	0.000	0.000	1.353	0.178	0.584
MDD or AnxD	-0.061	0.082	-0.751	0.454	0.791	-0.129	0.086	-1.492	0.138	0.533	-0.048	0.072	-0.665	0.507	0.791
MDD or AnxD*RRS total	0.001	0.001	0.510	0.611	0.791	0.002	0.001	1.283	0.201	0.603	0.000	0.001	0.361	0.719	0.846
Sex	0.000	0.013	0.025	0.980	0.980	-0.021	0.013	-1.561	0.121	0.533	-0.025	0.011	-2.228	0.027	0.420
Age	-0.001	0.001	-0.824	0.411	0.791	-0.003	0.001	-2.048	0.042	0.420	-0.001	0.001	-0.570	0.570	0.791
RRS reflection	0.002	0.002	1.004	0.317	0.766	0.001	0.002	0.487	0.627	0.791	0.002	0.001	1.475	0.142	0.533
MDD or AnxD	-0.031	0.059	-0.530	0.597	0.791	-0.061	0.063	-0.974	0.332	0.766	-0.012	0.052	-0.236	0.814	0.916
MDD or AnxD*RRS reflection	0.001	0.004	0.198	0.844	0.921	0.003	0.005	0.750	0.455	0.791	-0.001	0.004	-0.138	0.890	0.952
Sex	0.000	0.013	-0.035	0.972	0.980	-0.022	0.014	-1.584	0.115	0.533	-0.026	0.011	-2.303	0.023	0.420
Age	-0.001	0.001	-0.684	0.495	0.791	-0.002	0.001	-1.758	0.081	0.533	0.000	0.001	-0.375	0.709	0.846
RRS brooding	0.002	0.002	0.985	0.326	0.766	0.002	0.002	0.986	0.326	0.766	0.002	0.001	1.644	0.102	0.533
MDD or AnxD	-0.043	0.060	-0.713	0.477	0.791	-0.102	0.064	-1.601	0.111	0.533	-0.033	0.053	-0.611	0.542	0.791
MDD or AnxD*RRS brooding	0.002	0.004	0.385	0.701	0.846	0.006	0.005	1.330	0.185	0.584	0.001	0.004	0.223	0.824	0.916
Sex	0.002	0.013	0.121	0.904	0.952	-0.021	0.013	-1.566	0.120	0.533	-0.024	0.011	-2.139	0.034	0.420
Age	-0.001	0.001	-0.884	0.378	0.791	-0.003	0.001	-2.048	0.042	0.420	-0.001	0.001	-0.599	0.550	0.791
RRS depression related	0.000	0.001	0.292	0.771	0.890	0.000	0.001	0.543	0.588	0.791	0.001	0.001	1.020	0.309	0.766
MDD or AnxD	-0.062	0.088	-0.706	0.482	0.791	-0.124	0.092	-1.340	0.182	0.584	-0.058	0.077	-0.746	0.457	0.791
MDD or AnxD*RRS depression related	0.001	0.002	0.509	0.611	0.791	0.003	0.002	1.151	0.252	0.720	0.001	0.002	0.479	0.633	0.791

confidence interval for the difference not encompassing 0. However, it is important to highlight that this difference was not significant following correction for multiple comparisons. Therefore, our meta-analysis does not conclusively support these latter findings, although they have been reported in previous studies (Zhu et al., 2017).

Previous evidence suggests that the Core and DMPFC subsystems of the DMN contribute to different aspects of internal mentation (Andrews-Hanna, 2011). Specifically, the DMN Core acts as a network hub, integrating the function of the other subsystems. Activity in the DMN Core is also related to self-reports of personal significance, introspection about one's own mental states, and evoked emotion (Andrews-Hanna, 2011). The DMPFC subsystem, on the other hand, is primarily active when participants focus on their present mental state or when they infer the mental states of other people (Andrews-Hanna, 2011). Reduced neurotransmitters and volume have been reported in these regions in MDD previously and alterations in their function has been linked to symptoms, especially rumination (Zhu et al., 2017; Hasler et al., 2007; Khundakar and Thomas, 2009; Zhao et al., 2014). Interestingly, when considering DMN subsystems instead of the whole network, we found no significant difference between recurrent and first episode MDD. Also, we found no relationship between subsystems functional connectivity and current symptoms severity or illness duration. This suggests that decreased functional connectivity within and between the Core and DMPFC subsystems of the DMN might be a "trait" signature of MDD which persists from onset throughout the illness. However, the small effect size we detected for this difference significantly limits our ability

to interpret its neurobiological implications.

Our second contribution is to provide detailed meta-analysis metrics comparing the functional connectivity of DMN subsystems between MDD and healthy controls along with their relationship with symptom severity and clinical features. In particular, it is important to note that the effects we detected were small ( $g < 0.25$  for all significant effects) and, crucially, prediction intervals invariably encompassed 0. This mirrors the discrepant findings from the previous meta-analysis, which found increased connectivity in MDD and the most recent study by the Meta-MDD consortium, which found decreased connectivity (for meta-analysis: (Kaiser et al., 2015), for a multi-center study: (Yan et al., 2019)). Also, given that the effects were so weak and that prediction intervals encompassed 0, it was not surprising that we found no effect of MDD on DMN subsystems connectivity in our independently collected HCP-DES sample. These results are an important caveat for future work investigating the DMN in depression. For any study with this goal, large sample sizes are needed and even so, it is not guaranteed that there will be a detectable average effect on DMN functional connectivity when MDD is assumed to be a uniform diagnostic group and compared to healthy controls. Collaborative initiatives with open data sharing such as the Meta-MDD Consortium ([www.rfmri.org/REST-meta-MDD](http://www.rfmri.org/REST-meta-MDD)) and the NIH Human Connectome Studies Related To Disease (<https://www.humanconnectome.org/disease-studies>) will likely be key for finding robust effects of MDD and its subgroups on DMN functional connectivity.

Another important aspect revealed by our meta-analysis is that

**Table 6**

Results of linear regressions predicting DMN subsystem connectivity from rumination in the HCP-DES sample considering current MDD as a predictor. DMN = default mode network, DMPFC = dorsomedial prefrontal cortex, FC = functional connectivity, HC = healthy controls, MDD = major depressive disorder, FDR = false discovery rate, HCP-DES = human connectome project for disordered emotional states.

	DMN Core FC					DMN DMPFC FC					DMN Core-DMPFC FC				
	Coefficient	SE	t	p	pFDR	Coefficient	SE	t	p	pFDR	Coefficient	SE	t	p	pFDR
Sex	0.001	0.012	0.067	0.947	0.963	-0.020	0.013	-1.534	0.127	0.501	-0.025	0.011	-2.228	0.027	0.338
Age	-0.001	0.001	-0.858	0.392	0.811	-0.003	0.001	-2.021	0.045	0.338	-0.001	0.001	-0.567	0.571	0.897
RRS total	0.000	0.000	0.887	0.377	0.811	0.000	0.000	0.666	0.506	0.892	0.001	0.000	1.581	0.116	0.501
MDD	-0.040	0.073	-0.546	0.586	0.897	-0.114	0.077	-1.475	0.142	0.501	-0.030	0.064	-0.464	0.643	0.912
MDD*RRS total	0.000	0.001	0.238	0.812	0.961	0.002	0.001	1.254	0.212	0.606	0.000	0.001	0.092	0.927	0.961
Sex	0.001	0.012	0.089	0.929	0.961	-0.022	0.013	-1.636	0.104	0.501	-0.025	0.011	-2.263	0.025	0.338
Age	-0.001	0.001	-0.881	0.380	0.811	-0.003	0.001	-2.047	0.042	0.338	-0.001	0.001	-0.592	0.555	0.897
RRS reflection	0.002	0.002	1.079	0.282	0.677	0.001	0.002	0.731	0.466	0.892	0.003	0.001	1.775	0.078	0.468
MDD reflection	-0.034	0.053	-0.641	0.523	0.892	-0.022	0.056	-0.387	0.699	0.912	0.008	0.047	0.161	0.873	0.961
MDD*RRS reflection	0.001	0.004	0.236	0.814	0.961	0.001	0.004	0.135	0.893	0.961	-0.002	0.003	-0.621	0.535	0.892
Sex	-0.001	0.013	-0.104	0.917	0.961	-0.023	0.013	-1.701	0.091	0.496	-0.027	0.011	-2.437	0.016	0.338
Age	-0.001	0.001	-0.737	0.462	0.892	-0.002	0.001	-1.793	0.075	0.468	0.000	0.001	-0.433	0.666	0.912
RRS brooding	0.002	0.002	1.320	0.189	0.567	0.002	0.002	1.097	0.274	0.677	0.003	0.001	2.022	0.045	0.338
MDD brooding	-0.022	0.055	-0.402	0.689	0.912	-0.082	0.058	-1.414	0.159	0.530	-0.011	0.048	-0.220	0.826	0.961
MDD*RRS brooding	0.000	0.004	-0.034	0.973	0.973	0.005	0.004	1.096	0.275	0.677	-0.001	0.003	-0.287	0.775	0.961
Sex	0.001	0.012	0.115	0.908	0.961	-0.020	0.013	-1.498	0.136	0.501	-0.023	0.011	-2.120	0.036	0.338
Age	-0.001	0.001	-0.916	0.361	0.811	-0.003	0.001	-2.114	0.036	0.338	-0.001	0.001	-0.652	0.515	0.892
RRS depression related	0.000	0.001	0.528	0.598	0.897	0.000	0.001	0.397	0.692	0.912	0.001	0.001	1.135	0.258	0.677
MDD depression related	-0.028	0.072	-0.397	0.692	0.912	-0.118	0.076	-1.564	0.120	0.501	-0.044	0.063	-0.702	0.484	0.892
MDD*RRS depression related	0.000	0.002	0.122	0.903	0.961	0.003	0.002	1.363	0.175	0.553	0.001	0.002	0.359	0.720	0.919

results involving the Core subsystem were heterogeneous across sites. This heterogeneity might indicate the existence of discrete MDD subtypes characterized, for example, by a hypo-connected DMN Core and an intact DMN Core. It is known that with regards to its symptoms, depression can be quite heterogeneous (Fried and Nesse, 2015). In a synthesis of fMRI findings, we have previously highlighted the possibility that the diagnostic category of MDD arguably conflates underlying subtypes based on distinct neural circuit dysfunctions, including both hyper- and hypo-DMN connectivity (Williams, 2016). Therefore, future studies aiming to parse this clinical heterogeneity using functional connectivity measures, and the reverse, could focus on the DMN Core as a promising target. Further, heterogeneity for results involving the Core subsystem could be the consequence of other factors affecting its connectivity specifically, such as effects of different medication classes. For example, we have previously demonstrated that relatively intact Core DMN connectivity in untreated MDD characterizes patients who subsequently remit following treatment with commonly used antidepressants, whereas Core DMN hypo-connectivity characterizes patients who do not go on to remit on these antidepressants (Goldstein-Piekarski et al., 2018; Korgaonkar et al., 2020). It is possible therefore that available studies combine together treated patients who are both remitted and unremitted or untreated patients who will go on to be both remitters and non-remitters, and that these combined patients differ in their inherent DMN connectivity. These same patients may also be different in their inherent symptom profiles. Therefore, future fMRI studies of both predictive and mechanistic biomarkers of treatment could focus on the DMN Core and parse it from other DMN subsystems. Overall, we cannot draw conclusions from our meta-analysis about what might be driving the site heterogeneity for the Core connectivity results, therefore the above interpretations of the results remain speculative. Future studies could leverage the Meta-MDD dataset to test them or to identify site-specific confounding factors which might explain our results.

Finally, the last contribution from this study is to show that trait rumination as measured by the Rumination Response Scale is not a significant predictor of resting state functional connectivity within the DMN. This was true when investigating the Core and DMPFC subsystems, but also when conducting an exploratory analysis on all functional connections within the DMN. This null result was contrary to our original hypothesis and to previous studies on both MDD participants and healthy controls (Zhou et al., 2020; Greicius et al., 2007; Chen et al., 2020; Zhu et al., 2017; Lois and Wessa, 2016; R. and D, 2017). One potential explanation for our findings emerges from considering a previous study reporting a reliable correlation between functional connectivity between the DMN Core-DMPFC and trait rumination in a sample of healthy individuals (Chen et al., 2020). In that study, participants were asked to actively engage in a rumination and a distraction state during the scan. The correlation between Core-DMPFC functional connectivity and trait rumination was found specifically during the rumination state. Therefore, robust detection of this relationship might require active engagement of the DMN Core and DMPFC subsystems by a specific mentation state in contrast with task-free resting state. Indeed, it is even possible that different activation patterns during rumination between MDD and controls might drive the differences in functional connectivity that we detected. Another possibility extending upon the above points is that most studies assume MDD is a uniform entity rather than consider the heterogeneity of symptoms within the broader diagnosis. It may be of value to investigate whether trait rumination is characteristic of a distinct subgroup of MDD who also are also characterized by prominent disruptions in DMN connectivity, and to potentially explore if such a subgroup cuts across other diagnostic categories.

Our study is not without limitations. First of all, as outlined above, the lack of a tailored task designed to engage the DMN Core and DMPFC subsystems might have prevented us from detecting a relationship between their functional connectivity and trait rumination. Future studies

wishing to tackle this research question could consider such a design compared to task-free resting state. Secondly, our HCP-DES clinical sample consisted of untreated participants on a spectrum of depression and anxiety symptoms ranging from mild to severe. We believe this sample to be well-suited to study a transdiagnostic construct such as rumination, but we also acknowledge that reduced functional connectivity within and between DMN Core and DMPFC might be a feature specific to MDD. Another caveat is that acquisition parameters and, importantly, preprocessing of HCP-DES were different to the ones used in Meta-MDD. This could have induced systematic differences between the Meta-MDD and HCP-DES datasets that might have confounded our results. For example, connectivity values were higher in most of Meta-MDD sites compared to HCP-DES. We believe that this emphasizes the importance of evaluating the impact of methodological factors on putative illness biomarkers and that these should ideally be validated across different acquisition parameters and preprocessing streams. Finally, in our meta-analysis the number of frames containing motion correlated with the connectivity estimates. However, the effect was very small ( $g \sim 0.10$ ) and we also adopted a stringent criterion to remove subjects with excessive motion. Furthermore, the amount of motion did not differ between MDD and controls in our analyses.

To conclude, we show that MDD is characterized by slightly reduced functional connectivity in the resting state within the DMN Core. This is independent of illness duration, current symptoms and trait rumination. However, our results indicate that reduced mean Core DMN connectivity has significant limitations to be clinically useful or a promising neuropathological marker of MDD when MDD is assumed to be a homogenous diagnostic category: a small effect size, high variability, heterogeneity across samples and potential vulnerability to confounding factors. Since the effects we detected were very small and variability in the data is high, we recommend that future studies wishing to investigate functional connectivity differences in MDD use large datasets and that they investigate the existence of distinct subgroups that may be conflated within the broad diagnosis of MDD.

#### CRedit authorship contribution statement

**Leonardo Tozzi:** Conceptualization, Data curation, Formal analysis, Investigation, Methodology, Software, Project administration, Visualization, Writing - original draft, Writing - review & editing. **Xue Zhang:** Conceptualization, Writing - original draft, Writing - review & editing. **Megan Chesnut:** Investigation, Writing - review & editing. **Bailey Holt-Gosselin:** Investigation, Writing - review & editing. **Carolina A. Ramirez:** Data curation, Formal analysis, Writing - review & editing. **Leanne M. Williams:** Funding acquisition, Resources, Supervision, Writing - review & editing.

#### Declaration of Competing Interest

The authors declare that they have no known competing financial interests or personal relationships that could have appeared to influence the work reported in this paper.

#### Acknowledgements

Data were provided in part by the members of REST-meta-MDD Consortium.

#### Funding

This work was supported by the National Institutes of Health [grant number U01MH109985 under PAR-14-281].

#### Appendix A. Supplementary data

Supplementary data to this article can be found online at <https://doi.org/10.1016/j.nicl.2021.102570>.

[org/10.1016/j.nicl.2021.102570](https://doi.org/10.1016/j.nicl.2021.102570).

#### References

- Andrews-Hanna, J.R., Reidler, J.S., Sepulcre, J., Poulin, R., Buckner, R.L., 2010. Functional-anatomic fractionation of the brain's default network. *Neuron* 65, 550–562.
- Andrews-Hanna, J.R., 2011. The Brain's Default Network and Its Adaptive Role in Internal Mentation: The Neuroscientist DOI:10.1177/1073858411403316 (September 11, 2020).
- Brakowski, J., et al., 2017. Resting state brain network function in major depression - depression symptomatology, antidepressant treatment effects, future research. *J. Psychiatr. Res.* 92, 147–159.
- Chen, X., et al., 2020. The subsystem mechanism of default mode network underlying rumination: A reproducible neuroimaging study. *NeuroImage* 221, 117185.
- Chen, Y., Wang, C., Zhu, X., Tan, Y., Zhong, Y., 2015. Aberrant connectivity within the default mode network in first-episode, treatment-naïve major depressive disorder. *J. Affect. Disord.* 183, 49–56.
- Cox, R.W., Hyde, J.S., 1997. Software tools for analysis and visualization of fMRI data. *NMR Biomed.* 10, 171–178.
- Dale, A.M., Fischl, B., Sereno, M.I., 1999. Cortical surface-based analysis I. Segmentation and surface reconstruction. *Neuroimage* 9, 179–194.
- Esteban, O., et al., 2019. fMRIPrep: a robust preprocessing pipeline for functional MRI. *Nat. Methods* 16, 111–116.
- Fried, E.I., Nesse, R.M., 2015. Depression is not a consistent syndrome: an investigation of unique symptom patterns in the STAR\*D study. *J. Affect. Disord.* 172, 96–102.
- Friedrich, M.J., 2017. Depression is the leading cause of disability around the world. *JAMA* 317, 1517–1517.
- Glasser, M.F., et al., 2013. The minimal preprocessing pipelines for the Human Connectome Project. *Neuroimage* 80, 105–124.
- Goldstein-Piekarski, A.N., et al., 2018. Intrinsic functional connectivity predicts remission on antidepressants: a randomized controlled trial to identify clinically applicable imaging biomarkers. *Transl. Psychiatry* 8, 1–11.
- Greicius, M.D., et al., 2007. Resting-state functional connectivity in major depression: abnormally increased contributions from subgenual cingulate cortex and thalamus. *Biol. Psychiatry* 62, 429–437.
- Grisanzio, K.A., et al., 2018. Transdiagnostic symptom clusters and associations with brain, behavior, and daily function in mood, anxiety, and trauma disorders. *JAMA Psychiatry* 75, 201–209.
- Guo, W., et al., 2014. Abnormal default-mode network homogeneity in first-episode, drug-naïve major depressive disorder. *PLoS One* 9, e91102.
- Hamilton, M., 1959. The assessment of anxiety states by rating. *Br. J. Med. Psychol.* 32, 50–55.
- Hamilton, M., 1986. The Hamilton rating scale for depression. In: Sartorius, D.N., Ban, D. T.A. (Eds.), *Assessment of Depression*. Springer, Berlin Heidelberg, pp. 143–152.
- Hamilton, J.P., Farmer, M., Fogelman, P., Gotlib, I.H., 2015. Depressive rumination, the default-mode network, and the dark matter of clinical neuroscience. *Biol. Psychiatry* 78, 224–230.
- Hasler, G., et al., 2007. Reduced prefrontal glutamate/glutamine and gamma-aminobutyric acid levels in major depression determined using proton magnetic resonance spectroscopy. *Arch. Gen. Psychiatry* 64, 193–200.
- Iwabuchi, S.J., et al., 2015. Localized connectivity in depression: a meta-analysis of resting state functional imaging studies. *Neurosci. Biobehav. Rev.* 51, 77–86.
- Kaiser, R.H., Andrews-Hanna, J.R., Wager, T.D., Pizzagalli, D.A., 2015. Large-scale network dysfunction in major depressive disorder: a meta-analysis of resting-state functional connectivity. *JAMA Psychiatry* 72, 603–611.
- Khundakar, A.A., Thomas, A.J., 2009. Morphometric changes in early- and late-life major depressive disorder: evidence from postmortem studies. *Int. Psychogeriatr.* 21, 844–854.
- Korgaonkar, M.S., Goldstein-Piekarski, A.N., Fornito, A., Williams, L.M., 2020. Intrinsic connectomes are a predictive biomarker of remission in major depressive disorder. *Mol. Psychiatry* 25, 1537–1549.
- Lois, G., Wessa, M., 2016. Differential association of default mode network connectivity and rumination in healthy individuals and remitted MDD patients. *Soc. Cogn. Affect. Neurosci.* 11, 1792–1801.
- Mor, N., Winquist, J., 2002. Self-focused attention and negative affect: a meta-analysis. *Psychol. Bull.* 128, 638–662.
- Mulders, P.C., van Eijndhoven, P.F., Schene, A.H., Beckmann, C.F., Tendolcar, I., 2015. Resting-state functional connectivity in major depressive disorder: a review. *Neurosci. Biobehav. Rev.* 56, 330–344.
- Nolen-Hoeksema, S., Wisco, B.E., Lyubomirsky, S., 2008. Rethinking rumination. *Perspect. Psychol. Sci.* 3, 400–424.
- Ochsner, K.N., et al., 2004. Reflecting upon feelings: an fMRI study of neural systems supporting the attribution of emotion to self and other. *J. Cogn. Neurosci.* 16, 1746–1772.
- Ogawa, S., Lee, T.-M., 1990. Magnetic resonance imaging of blood vessels at high fields: in vivo and in vitro measurements and image simulation. *Magn. Reson. Med.* 16, 9–18.
- Parola, N., et al., 2017. Psychometric properties of the Ruminative Response Scale-short form in a clinical sample of patients with major depressive disorder. *Patient Prefer. Adherence* 11, 929–937.
- Power, J.D., et al., 2011. Functional network organization of the human brain. *Neuron* 72, 665–678.
- Power, J.D., et al., 2014. Methods to detect, characterize, and remove motion artifact in resting state fMRI. *NeuroImage* 84, 320–341.

- Pruim, R.H.R., et al., 2015. ICA-AROMA: a robust ICA-based strategy for removing motion artifacts from fMRI data. *Neuroimage* 112, 267–277.
- Rosenbaum, D., et al., 2017. Aberrant functional connectivity in depression as an index of state and trait rumination. *Sci. Rep.* 7, 2174–2174.
- Schaefer, A., et al., 2018. Local-global parcellation of the human cerebral cortex from intrinsic functional connectivity MRI. *Cereb. Cortex* 28, 3095–3114.
- Schwarzer, G., Carpenter, J.R., Rücker, G., 2015. *Meta-Analysis with R* (Springer International Publishing, 2015) DOI:10.1007/978-3-319-21416-0.
- Setsompop, K., et al., 2012. Blipped-controlled aliasing in parallel imaging for simultaneous multislice echo planar imaging with reduced g-factor penalty. *Magn. Reson. Med.* 67, 1210–1224.
- Tang, S., et al., 2018. Abnormal amygdala resting-state functional connectivity in adults and adolescents with major depressive disorder: a comparative meta-analysis. *EBioMedicine* 36, 436–445.
- Thomas Yeo, B.T., et al., 2011. The organization of the human cerebral cortex estimated by intrinsic functional connectivity. *J. Neurophysiol.* 106, 1125–1165.
- Tozzi, L., et al., 2020. The human connectome project for disordered emotional states: protocol and rationale for a research domain criteria study of brain connectivity in young adult anxiety and depression. *NeuroImage* 214, 116715.
- Treynor, W., Gonzalez, R., Nolen-Hoeksema, S., 2003. Rumination reconsidered: a psychometric analysis. *Cognitive Ther. Res.* 27, 247–259.
- Veroniki, A.A., et al., 2016. Methods to estimate the between-study variance and its uncertainty in meta-analysis. *Res. Synth. Methods* 7, 55–79.
- Williams, L.M., 2016. Precision psychiatry: a neural circuit taxonomy for depression and anxiety. *Lancet Psychiatry* 3, 472–480.
- Yan, C.-G., et al., 2019. Reduced default mode network functional connectivity in patients with recurrent major depressive disorder. *PNAS* 116, 9078–9083.
- Zalesky, A., Fornito, A., Bullmore, E.T., 2010. Network-based statistic: identifying differences in brain networks. *NeuroImage* 53, 1197–1207.
- Zhao, Y.-J., et al., 2014. Brain grey matter abnormalities in medication-free patients with major depressive disorder: a meta-analysis. *Psychol. Med.* 44, 2927–2937.
- Zhou, H.-X., et al., 2020. Rumination and the default mode network: Meta-analysis of brain imaging studies and implications for depression. *NeuroImage* 206, 116287.
- Zhu, X., Zhu, Q., Shen, H., Liao, W., Yuan, F., 2017. Rumination and default mode network subsystems connectivity in first-episode, drug-naive young patients with major depressive disorder. *Sci. Rep.* 7, 43105.